



Reprint Order Form—Norwell Titles

Professionally produced reprints of your article will be available upon publication. Authors will receive 25 reprints free of charge. To facilitate this, please complete and return this form to address listed on the order page. If you wish to purchase reprints, use the grid below to determine the price based on page-length and number of reprints ordered. If your article contains color images and you wish for it to be reproduced in color, please refer to the "Color Articles" pricing below. However, you may choose to have those color images reproduced in black & white only by referring to the "Black & White Articles" pricing.

IMPORTANT:

1. You must clearly indicate if you wish to have full "COLOR" reproduction. Prompt return will ensure a quicker delivery of your reprints.
2. Orders that are received without payment will NOT be processed. Please remember to include your check or credit card information with your order.
3. If you do not know your page count at this time, please fill out as much of the form as possible and return to the address listed. You will be notified upon your article's publication.

Articles are printed on high quality paper. Page counts over four are saddle stitched in booklet format. Reprints are available with or without covers. Please allow 4-6 weeks from the print publication date for delivery. Articles are not fully print-formatted until just before their publication in print. Thus, to ensure the highest quality reprints possible, an article's reprint availability coincides with its print publication.

Black & White Articles—8 ½ X 11 Trim Size							
Qty.	No. of Pages						
	1-2	3-4	5-8	9-12	13-16	17-20	21-24
100 min.	\$136	\$232	\$444	\$632	\$812	\$1,008	\$1,184
200	\$148	\$256	\$492	\$708	\$904	\$1,124	\$1,320
300	\$156	\$276	\$544	\$780	\$996	\$1,240	\$1,460
400	\$168	\$300	\$592	\$852	\$1,092	\$1,356	\$1,600
500	\$180	\$324	\$644	\$924	\$1,184	\$1,472	\$1,736

Color Articles—up to 8 ½ X 11 Trim Size							
Qty.	No. of Pages						
	1-2	3-4	5-8	9-12	13-16	17-20	21-24
100 min.	\$262	\$414	\$827	\$1,218	\$1,502	\$1,743	\$1,900
200	\$293	\$468	\$902	\$1,337	\$1,653	\$1,929	\$2,230
300	\$317	\$500	\$979	\$1,491	\$1,860	\$2,149	\$2,500
400	\$338	\$542	\$1,062	\$1,579	\$1,972	\$2,283	\$2,662
500	\$353	\$575	\$1,135	\$1,671	\$2,099	\$2,416	\$2,814

Optional Covers: Vellum cover with article title, author name and reprint line	100	200	300	400	500
	\$62	\$70	\$78	\$86	\$94

Ordering Information:

All orders must be paid in advance by check, money order, Visa, MasterCard or American Express. If paying by check or money order, the funds should be drawn on a U.S. Bank and payable in U.S. dollars to **Sheridan Reprints**. Domestic orders will be shipped via UPS-ground service. International orders will be shipped via International Air Courier. Please see chart for freight pricing information. If you prefer a different shipping method, or have any questions about your order, please contact **Lori Sentz at 800-352-2210 ext. 8134 or email lsentz@tsp.sheridan.com**

Mail this form to: Springer, 101 Philip Drive, Norwell, MA 02061,
Attn: Katie Costello or email at katie.costello@springer-sbm.com
Or Fax form to: (781) 871-6848 Attn: Katie Costello

Order Form

Please place my order for—**Journal of Materials Science**

Article Title: _____ Article #: _____

Author: _____

Page Total: _____ Article begins on page # _____ and ends on page # _____

Are you requesting color reprints? YES NO If yes, you must be sure to use the color pricing grid and indicate color in the order section

*If you do not know your page count at this time, please fill out as much of the form as possible and return to the address listed. You will be notified upon your article's publication.

I am not ordering additional reprints at this time, but please use the shipping information below to facilitate the processing of my Gratis order.

Bill To: Name: (please print) _____

Company: _____

Address: _____

City/State/Zip: _____

Phone: (include area code) _____

E-MAIL: (please print) _____

Signature: _____

Ship To: Name: (please print) _____

Company/Dept: _____

Address: _____

Address: _____

City/State/Zip: _____

Country: _____

Phone: (include area code) _____

E-MAIL: (please print) _____

Author Complimentary (gratis) copies: 25 FREE

Number of additional Reprints Ordered: _____ \$ _____

Have you selected the appropriate B&W or Color pricing and entered above?

Covers: Yes..... NO..... \$ _____

Shipping: (see below) _____ \$ _____

Total \$ _____

Shipping Information:

Domestic orders-UPS ground, add: \$16.00

International orders-Air Courier Service

If your order is 8 pages or less or 200 copies or less, add:\$75.00

If your order is more than 8 pages or more than 200 copies, add: ...\$105.00

If you have any questions, please call Lori Sentz at 800-352-2210 ext. 8134 or email

lsentz@tsp.sheridan.com

Method of Payment

(check one box)

Payment Enclosed

Check or Money Order Only

Make payable to Sheridan Reprints

In U.S. Funds only



If paying by credit card, do you require a receipt?

If so, please enter fax # or email address below.

CARD NUMBER

_____ - _____ - _____ - _____

Expiration Date ____ - ____

Signature _____

PRINT Cardholder's Name _____

*Payments made by credit card are not processed for payment until your article enters production. Payments made by check or money order are deposited immediately upon receipt for security purposes. However, the article will not enter the production cycle until after it has been published.

Journal of Materials Science Keyword Thesaurus

Please select three (or fewer) keywords for your paper from the list below and return this form with your correct
Please note that these keywords are not used to compile the annual index, but are for contents use only.

adhesion
 adsorption
 amorphous materials
 anisotropy
 annealing
 biomaterials
 blends
 bonding
 brazing
 casting
 catalysts
 cellular materials
 ceramics
 characterization methods
 chemical vapour deposition
 coatings
 composite materials
 computer simulation
 corrosion and oxidation
 crystal growth
 crystallization
 crystallographic texture
 curing
 defects
 deformation and fracture
 deposition techniques
 diffusion
 elastic properties
 electrical properties
 electrochemistry
 electron beam techniques
 electronic materials
 electronic properties
 electronic materials
 epitaxial growth
 fatigue
 ferroelectrics
 fibre technology
 filter
 fracture
 functionally graded materials
 gas phase transport
 gelation
 glasses
 grain boundaries
 grooves
 hardness
 healing
 heat treatment
 high-temperature superconductors
 hot isostatic pressing
 hydrolysis
 imaging
 infrared spectroscopy
 intercalation
 interfaces
 intermetallic alloys & compounds

kinetics
 laminates
 laser processing
 latticed effects
 lithography
 machining
 macro defects
 magnetic materials
 magnetostatic properties
 mechanical properties
 mercury cadmium telluride
 metals and alloys
 microanalysis
 microstructure
 mineral
 mineralization
 modelling
 moulding
 multilayer structure
 nanocomposites
 nanomaterials
 neutronic
 neutronic radioactivation
 nondestructive testing
 nonlinear properties
 nuclear magnetic resonance
 optical materials and properties
 organic compounds
 ossification
 phase diagrams
 phase transformations
 photoreactive materials
 piezoelectric materials
 plasma deposition
 plating
 polymers
 porosity
 powder technology
 rapidly solidified materials
 semiconductors
 simulations
 sintering
 smart materials
 sol-gel preparation
 solidification
 sputter deposition
 superconductors
 surfaces
 surfactant
 tendon
 thermal properties
 thin and thick film coatings
 transmission
 transport mechanism
 tribology
 viscoelasticity
 viscosity

wear
 X-ray techniques

Insert JMSC article number here:

Metadata of the article that will be visualized in OnlineFirst

ArticleTitle	Formation of boride layers at the Fe–25% Cr alloy–boron interface	
Journal Name	Journal of Materials Science	
Corresponding Author	Family Name	Dybkov
	Particle	
	Given Name	V. I.
	Suffix	
	Organization	Institute for Problems of Materials Science
	Division	Department of Physical Chemistry of Inorganic Materials
	Address	03180, Kyiv, Ukraine
	Email	vdybkov@ukr.net
Author	Family Name	Lengauer
	Particle	
	Given Name	W.
	Suffix	
	Organization	Vienna University of Technology
	Division	Institute for Chemical Technologies and Analytics
	Address	1060, Vienna, Austria
	Email	
Author	Family Name	Gas
	Particle	
	Given Name	P.
	Suffix	
	Organization	L2MP-CNRS, Faculté des Sciences St Jerome
	Division	
	Address	Case 142, 13397, Marseille, France
	Email	
Schedule	Received	21 April 2005
	Revised	
	Accepted	22 September 2005
Abstract	<p>Two boride layers based on the FeB and Fe₂B compounds are formed at the interface between a Fe–25% Cr alloy and boron at 850–950 °C and reaction times up to 12 h. The characteristic feature of both layers is a pronounced texture. Each of two boride layers is compositionally two-phase. The outer layer consists of the (Fe,Cr)B and (Cr,Fe)B phases. The inner layer comprises the (Fe,Cr)₂B and (Cr,Fe)₂B phases. The diffusional layer-growth kinetics are close to parabolic and can alternatively be described by a system of two non-linear differential equations, also producing a fairly good fit to the experimental data. Annealing of a borided Fe–Cr sample in the absence of boriding media results in the disappearance of the (Fe,Cr)B–(Cr,Fe)B layer, with the (Fe,Cr)B phase disappearing first. Microhardness values are 21.0 GPa for the outer layer, 18.0 GPa for the inner layer and 1.35 GPa for the alloy base. The abrasive wear resistance of the (Fe,Cr)B–(Cr,Fe)B layer, found from mass loss measurements, is more than 150 times greater than that of the alloy base.</p>	
Keywords	Fe–25% Cr alloy - Boron - Boride layers - Phase identity - Chemical composition - Growth kinetics - Abrasive wear resistance	
Footnote Information		

3 **Formation of boride layers at the Fe–25% Cr alloy–boron**
4 **interface**

V. I. Dybkov · W. Lengauer · P. Gas

5

6

7 Received: 21 April 2005 / Accepted: 22 September 2005 / Published online: ■

8 © Springer Science+Business Media, LLC 2006

9

10 **Abstract** Two boride layers based on the FeB and Fe₂B
11 compounds are formed at the interface between a Fe–25%
12 Cr alloy and boron at 850–950 °C and reaction times up to
13 12 h. The characteristic feature of both layers is a pro-
14 nounced texture. Each of two boride layers is composi-
15 tionally two-phase. The outer layer consists of the (Fe,Cr)B
16 and (Cr,Fe)B phases. The inner layer comprises the
17 (Fe,Cr)₂B and (Cr,Fe)₂B phases. The diffusional layer-
18 growth kinetics are close to parabolic and can alternatively
19 be described by a system of two non-linear differential
20 equations, also producing a fairly good fit to the experi-
21 mental data. Annealing of a borided Fe–Cr sample in the
22 absence of boriding media results in the disappearance of
23 the (Fe,Cr)B–(Cr,Fe)B layer, with the (Fe,Cr)B phase
24 disappearing first. Microhardness values are 21.0 GPa for
25 the outer layer, 18.0 GPa for the inner layer and 1.35 GPa
26 for the alloy base. The abrasive wear resistance of the
27 (Fe,Cr)B–(Cr,Fe)B layer, found from mass loss measure-
28 ments, is more than 150 times greater than that of the alloy
29 base.

30

Introduction

31

Boriding is one of the widespread thermochemical surface
32 treatments used to improve service characteristics (hard-
33 ness, mechanical and corrosive wear resistance, etc.) of
34 steels, metals and alloys [1–3]. Iron borides Fe₂B and FeB
35 are known to exist in the Fe–B binary system [4–7].
36 Therefore, with iron, its alloys and steels, either one-phase
37 or two-phase coatings can be obtained, depending on
38 boriding techniques employed and temperature-time con-
39 ditions of a boriding procedure. 40

It is worth mentioning that even if three or more
41 compounds exist in the metal–boron binary system, in
42 most cases only two of them form separate layers at the
43 interface between reacting phases [8]. This contradicts
44 diffusional considerations [9] predicting the simultaneous
45 formation and subsequent parabolic growth of the layers
46 of all compounds of any binary system, whatever their
47 number, but agrees with a physicochemical viewpoint
48 [10], according to which one or two layers can occur and
49 grow simultaneously under conditions of diffusion con-
50 trol, with other compound layers being skipped for kinetic
51 reasons. 52

The properties of boride coatings are to a large extent
53 dependent on the amount of alloying elements and
54 impurities present in the base material. In the case of
55 materials of complicated chemical composition, for
56 example steels, it is not so easy to separate the effect of a
57 particular element from that of others. Therefore, exper-
58 iments with binary alloys are desirable. In this work, the
59 results of the experimental investigation of the interaction
60 of an Fe–25%Cr alloy with boron at 850–950 °C are
61 presented. 62

V. I. Dybkov (✉)
Department of Physical Chemistry of Inorganic Materials,
Institute for Problems of Materials Science, Kyiv 03180, Ukraine
e-mail: vdybkov@ukr.net

W. Lengauer
Institute for Chemical Technologies and Analytics, Vienna
University of Technology, 1060 Vienna, Austria

P. Gas
L2MP-CNRS, Faculté des Sciences St Jerome, Case 142, 13397
Marseille, France

63 **Experimental procedure**64 **Materials and specimens**

65 The materials used were high-purity carbonyl iron powder
66 (99.98% Fe), electrolytic-grade chromium platelets
67 (99.98% Cr), amorphous boron and analytical-grade KBF_4 .
68 Initially, the boron powder contained 98.3% B, 0.04% C,
69 1.6% O and insignificant amounts of Si, Cu, Mg (<0.01%
70 each) and Fe (<0.001%). Before the boriding experiments,
71 the powder was first heated slowly in vacuum up to
72 1450 °C and then calcined at this temperature for 2 h in an
73 atmosphere of argon at a pressure of 2.5×10^4 Pa to remove
74 volatile oxides. KBF_4 was preliminary dried in steps at 95,
75 110, 130 and 170 °C (24 h at each temperature).

76 Cylindrical rods of an Fe–25% Cr alloy, about 13 mm in
77 diameter and 100 mm long, were prepared by arc-melting
78 of appropriate metals under argon, with subsequent casting
79 of the melts into water-cooled copper crucibles. The rods
80 were annealed to ensure their homogenization at a tem-
81 perature of 1100 °C for 2 h in an argon atmosphere at a
82 pressure of 2.5×10^4 Pa. From these, Fe–Cr alloy speci-
83 mens in the form of tablets, 11.28 mm diameter and
84 5.5 mm high, were machined. Flat sides (1 cm² area) of the
85 tablets were ground and polished mechanically.

86 **Methods**

87 The boriding procedure was performed using a vacuum
88 device VPBD-2S consisting of a high-vacuum chamber with
89 a molybdenum-sheet electric-resistance furnace (tempera-
90 tures up to 1600 °C) and a control panel. The experiment was
91 carried out in an alumina crucible, 13 mm inner diameter and
92 40 mm high. An iron–chromium alloy tablet was embedded
93 into a mixture of boron powder with 5% KBF_4 as an
94 activator. This amount of KBF_4 appears to be optimum [1, 8].
95 The mixture was then slightly pressed, and a load of 8.5 g
96 (a low-carbon steel cylinder) was placed on top. The crucible
97 was closed with a low-carbon steel lid and placed into a steel-
98 sheet holder, mounted to a guide rod capable of moving in the
99 vertical direction.

100 The chamber was pumped to a pressure of about 10 Pa
101 and filled with high-purity argon (99.999 vol.% Ar). This
102 procedure was repeated twice. Then, the chamber was
103 again pumped and filled with argon at a pressure of
104 2.5×10^4 Pa, and heating was started. During heating, the
105 crucible with its contents was in the cold zone above the
106 furnace.

107 After the required temperature in the range of 850–
108 950 °C had been reached in the furnace, the crucible, pre-
109 heated to about 400 °C, was moved into its middle part.

After an initial drop, the temperature attained its pre- 110
determined value in 4–5 min and was then maintained 111
constant within ± 1 °C with the help of an automatic ther- 112
moregulator VRT-3. The temperature measurements were 113
carried out using a Pt–PtRh thermocouple. The experi- 114
ments were carried out at temperatures of 850, 900 and 115
950 °C. Their duration was 3,600–43,200 s (1–12 h). 116

After the experiment, the Fe–Cr alloy tablet coated with 117
boride layers was cut along the cylindrical axis into two 118
unequal parts (7 mm and 4 mm) using an electric-spark 119
machine. The greater part of the tablet was embedded into 120
a cold-setting epoxy resin and used to prepare a metallo- 121
graphic cross-section. The lesser part was used for X-ray 122
diffraction investigations (plain-view samples). 123

Characterization of Fe–Cr alloys and boride layers was 124
carried out with the help of metallography, X-ray (XA) and 125
chemical (CA) analyses, and electron probe microanalysis 126
(EPMA). The composition of the Fe–Cr alloy prepared was 127
found by CA and EPMA to correspond to a nominal value 128
of 25% Cr within $\pm 0.4\%$. Its constituting phase was shown 129
by XA to be the α -phase. 130

The thickness of boride layers was measured using an 131
optical microscope MIM-7 equipped with a HP Photosmart 132
720 camera. The chemical composition of the layers and 133
the concentration profiles of the elements in the transition 134
zone between reacting phases were obtained using electron 135
probe microanalyzers JEOL Superprobe 733 and CAME- 136
CA Camebax SX50. The beam spot diameter and the phase 137
volume analyzed at each point were estimated to be about 138
1 μm and 2 μm^3 , respectively. 139

X-ray diffraction patterns were taken immediately from 140
the surface of tablet samples on a DRON-3 apparatus using 141
 CuK_α radiation. When taking the first pattern, no polishing 142
of a borided Fe–Cr alloy sample was applied (section 0). 143
Then, about 10 μm of a boride layer was removed by 144
grinding and subsequent polishing, and another X-ray dif- 145
fraction pattern was taken (section I). This procedure was 146
repeated at a step of 10–40 μm until the Fe–Cr alloy base 147
was reached (sections II–VI). Seven X-ray diffraction 148
patterns were thus taken on each borided Fe–Cr sample. 149

Microhardness measurements on metallographic cross- 150
sections were carried out using a PMT-3 tester with the 151
diamond pyramide. The load was 0.98 N (100 g). 152

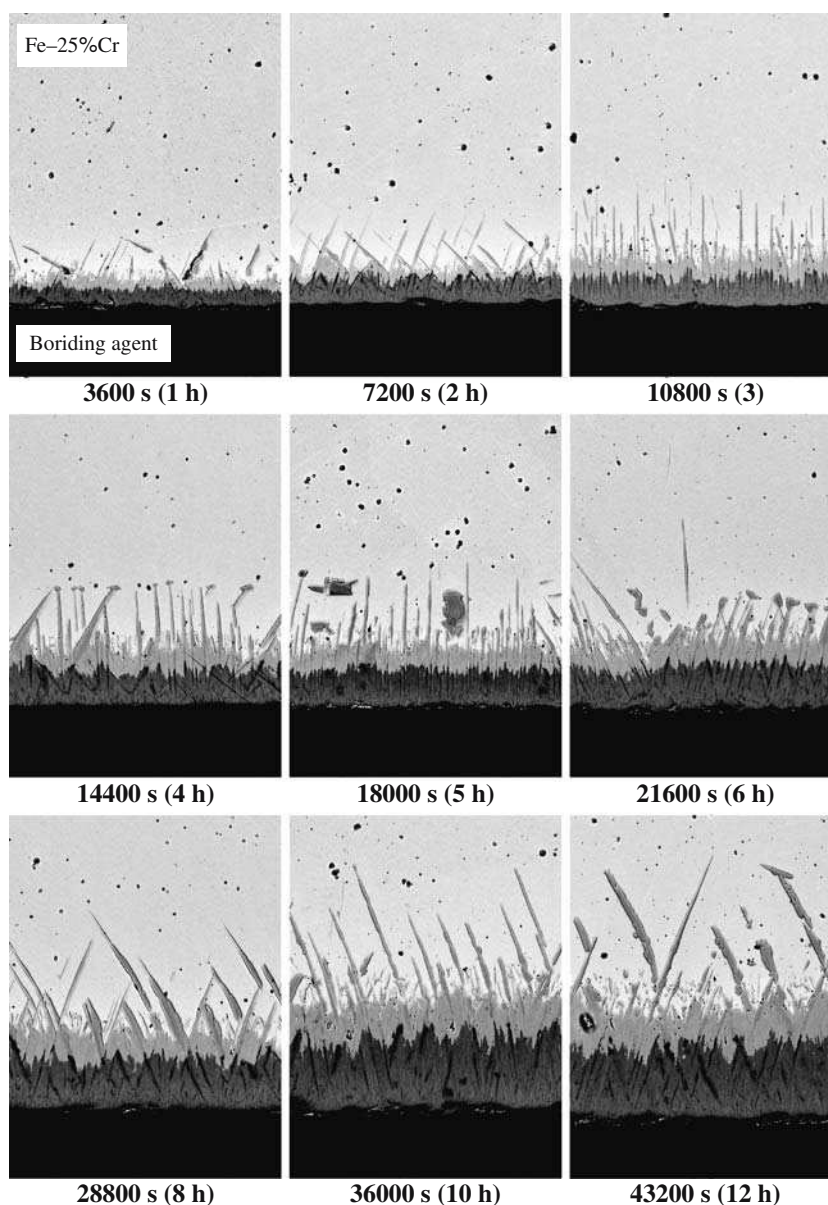
Abrasive wear resistance tests were carried out on P180 153
silicon carbide emery paper tape (main fraction grain size 154
63 μm , maximum 90 μm) using an AWRD-5 device. The 155
velocity of continuous movement of the tape (30 m long) 156
was 0.35 m s⁻¹, while the sliding distance during each test 157
was 27.0 m. The load was 50 N (5.1 kg). The working area 158
of tablet samples was 1 cm². The wear resistance of boride 159
layers and the alloy base was determined by means of 160
weighing the samples and measuring their height. 161

162 **Results and discussion**163 Phase identity and chemical composition of boride
164 layers

165 Two boride phases were found to occur as separate layers
166 at the interface between an Fe–25% Cr alloy and boron at
167 850–950 °C and reaction times up to 12 h, as illustrated in
168 Fig. 1. Layer-by-layer X-ray diffraction analysis (Fig. 2)
169 and a further comparison of our and literature [11] data
170 showed the outer layer bordering the boriding agent to be
171 the FeB phase and the inner layer adjacent to the Fe–Cr
172 alloy base to be the Fe₂B phase (Fig.3 and Tables 1 and 2).

173 As seen from cross-sectional micrographs in Figs. 1 and
174 2, both layers consist of columnar crystals oriented pre-
175 ferentially in the direction of diffusion or at an angle of 20°–
176 25° to this direction. Their characteristic feature is a pro-
177 nounced texture. The strongest reflections are {002}
178 ($2\theta = 63.4^\circ$ and spacing, $d = 0.148$ nm) and, to a lesser
179 extent, {020} ($2\theta = 32.5^\circ$ and $d = 0.275$ nm) for the
180 orthorhombic FeB phase, and {002} ($2\theta = 42.8^\circ$ and
181 $d = 0.212$ nm) for the tetragonal Fe₂B phase, in agreement
182 with findings of other researchers [1, 12–14]. The change
183 in intensities of those reflections with increasing distance
184 from the surface of a borided Fe–25% Cr alloy tablet is
185 shown in Fig.4 and Table 3.

Fig. 1 Backscattered electron images of boride layers formed at the Fe–25% Cr alloy–boron interface at a temperature of 950 °C. Layer-by-layer X-ray analysis showed the darker layer bordering the boriding agent to be the FeB phase and the brighter layer adjacent to the Fe–Cr alloy base to be the Fe₂B phase



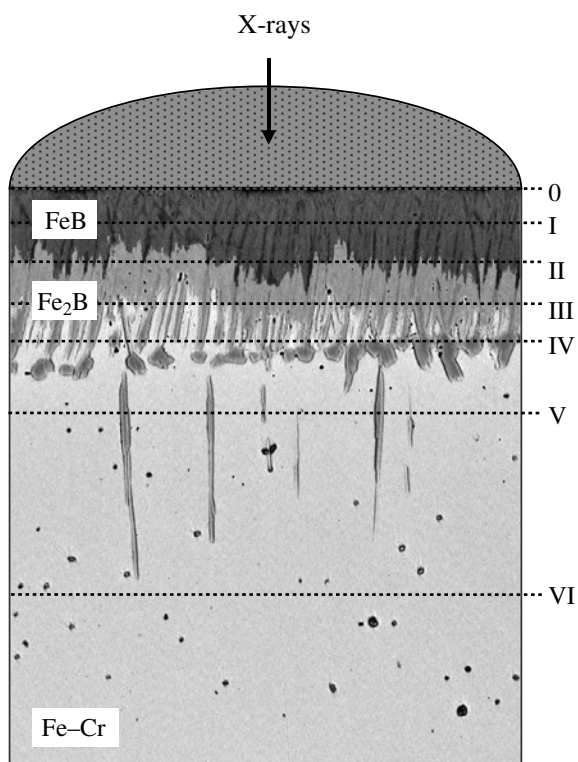


Fig. 2 Scheme of X-ray diffraction experiments

186 As evidenced in Fig.4 and Table 3 (see also Fig. 2), the
 187 larger orientation order (higher peak intensity) is charac-
 188 teristic of the inner portions of both boride layers compared
 189 to their near-interface portions. This is easily explainable
 190 because near-interface portions of any boride layer are less
 191 equilibrated compared to its inner portions. Therefore,

192 near-interface crystals have less time to align in the pre-
 193 ferred direction. The boride layer ordering process has been
 194 considered in detail by Voroshnin and Lyakhovich [1] and
 195 recently by Martini et al. [14] (see Fig. 3 of their paper).

196 X-ray investigations were followed by EPMA mea-
 197 surements (Table 4). Sections 0 and I of a borided Fe–Cr
 198 sample seem to correspond to a single-phase region (see
 199 Fig. 2). However, even though with iron, its alloys and
 200 steels a boride layer bordering the boriding agent is con-
 201 ventionally considered to consist of the FeB phase [1] and
 202 our X-ray diffraction data provide the strong support to this
 203 view-point, its microstructure (Fig. 5) and chemical com-
 204 position (Table 4) is in fact more complicated. As seen
 205 from plain-view micrographs of Fig. 5, the outer boride
 206 layer consists of distinct brighter and darker regions, with
 207 the latter having a peculiar regular arrangement. EPMA
 208 measurements in Table 4 indicate that iron prevails in
 209 brighter regions, while chromium is dominant in darker
 210 regions.

211 Hence, compositionally the outer boride layer actually
 212 comprises the (Fe,Cr)B and (Cr,Fe)B phases, although
 213 X-ray diffraction analysis does not show the presence of
 214 the CrB phase, probably because, firstly, the FeB and CrB
 215 phases have very similar crystal structures [4–6, 11] and,
 216 secondly, under non-equilibrium conditions the lattice
 217 rearrangement is not completed in view of time limita-
 218 tions. Being far from equilibrium, this layer appears to be
 219 single-phase structurally and two-phase compositionally.
 220 Since the scan line in Fig. 6 crosses areas of different
 221 chemical composition (even within the same boride
 222 phase), it is not surprising that the cross-sectional con-

Fig. 3 X-ray diffraction patterns of the FeB and Fe₂B phases. Boriding conditions: temperature 950 °C, reaction time 21,600 s (6 h)

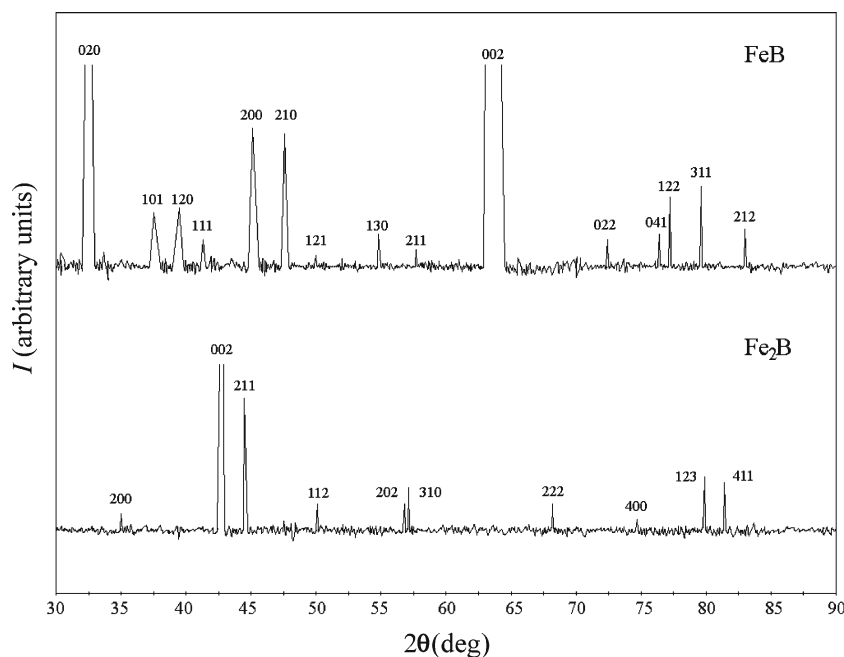


Table 1 Comparison of literature and our experimental X-ray data (*d*-spacing and peak intensities) for the FeB phase formed at the interface between an Fe–25% Cr alloy and boron at 950 °C and a reaction time of 21600 s (6 h)

Literature data [11]			Experimental data		
<i>HKL</i>	<i>d</i> (nm)	<i>I</i> ^a	2θ (deg)	<i>d</i> (nm)	<i>I</i>
020	0.275	s	32.5	0.2752	vs
101	0.240	s	37.3	0.2410	m
120	0.228	s	39.5	0.2281	m
111	0.219	vs	41.3	0.2186	w
200; 021	0.201	vs	45.1	0.2010	vs
210	0.190	vs	47.6	0.1910	s
121	0.181	s	50.0	0.1811	vw
130	0.167	s	54.8	0.1675	w
211	0.160	s	57.7	0.1597	vw
002	0.148	m	63.4	0.1467	vs
022	0.1303	m	72.4	0.1305	w
041	0.1249	m	76.4	0.1246	w
122	0.1239	vs	77.2	0.1236	m
311	0.1199	m	79.6	0.1204	m
212	0.1166	vs	83.0	0.1163	w

^aIntensity: vw, very weak; w, weak; m, medium; s, strong; vs, very strong

Table 2 Comparison of literature and our experimental X-ray data (*d*-spacing and peak intensities) for the Fe₂B phase formed at the interface between an Fe–25% Cr alloy and boron at 950 °C and a reaction time of 21600 s (6 h)

Literature data [11]			Experimental data		
<i>HKL</i>	<i>d</i> (nm)	<i>I</i> ^a	2θ (deg)	<i>d</i> (nm)	<i>I</i>
200	0.256	vw	35.0	0.2549	vw
002	0.212	w	42.8	0.2113	vs
211	0.201	vs	44.5	0.2014	vs
112	0.183	m	50.1	0.1831	w
202	0.163	m	56.8	0.1628	w
310	0.161	m	57.1	0.1615	m
222	0.1371	w	68.2	0.1375	w
400	0.1277	m	74.7	0.1272	vw
123	0.1202	s	79.9	0.1199	m
411	0.1187	m	81.4	0.1182	m

^aIntensity: vw, very weak; w, weak; m, medium; s, strong; vs, very strong

223 centration profiles of the elements Fe, Cr and B are so
224 irregular, except iron and chromium profiles in the alloy
225 base.

226 As seen in Fig. 2 and Table 3, section II crossed both
227 the FeB and Fe₂B layers, whereas section III crossed the
228 Fe₂B layer and partially the alloy base. The Fe₂B layer
229 was also found to be non-homogeneous (Fig. 7). Like the
230 FeB layer, it consists of the (Fe,Cr)₂B phase (region A in
231 Fig. 7, see also Table 4) and the (Cr,Fe)₂B phase (region
232 B). Note that the Fe₂B and Cr₂B phases are isomorphous
233 [4–6, 11].

234 The microstructure of sections IV and V consists of the
235 (Cr,Fe)₂B phase in the decreasing amount and the alloy
236 base somewhat depleted in chromium (Fig. 8 and Table 4).
237 Section VI is entirely the alloy base of an initial compo-
238 sition of 25% Cr.

Microhardness of boride phases 239

Microhardness, HV₁₀₀, of the outer (Fe,Cr)B–(Cr,Fe)B 240
layer was found to be 21.0 ± 2.0 GPa, while that of the 241
inner (Fe,Cr)₂B–(Cr,Fe)₂B layer to be 18.0 ± 1.0 GPa. For 242
the Fe–25% Cr alloy base, its value is 1.35 ± 0.09 GPa. 243

Microhardness values vary considerably within both 244
boride layers in view of their non-homogeneity. The dif- 245
ference in microhardness of near-boride and far-away 246
Fe–Cr regions is insignificant (about 0.1 GPa). 247

Layer-growth kinetics 248

Even though the boride layers are rather irregular, it is 249
possible to extract some kinetic data from the experimental 250
results obtained. With the ragged inner boride layer, the 251

Fig. 4 Most intensive peaks of X-ray diffraction patterns taken from different plain-view sections of an Fe–25% Cr alloy sample borided at 950 °C for 21600 s (6 h) (see also Fig. 2 and Table 3)

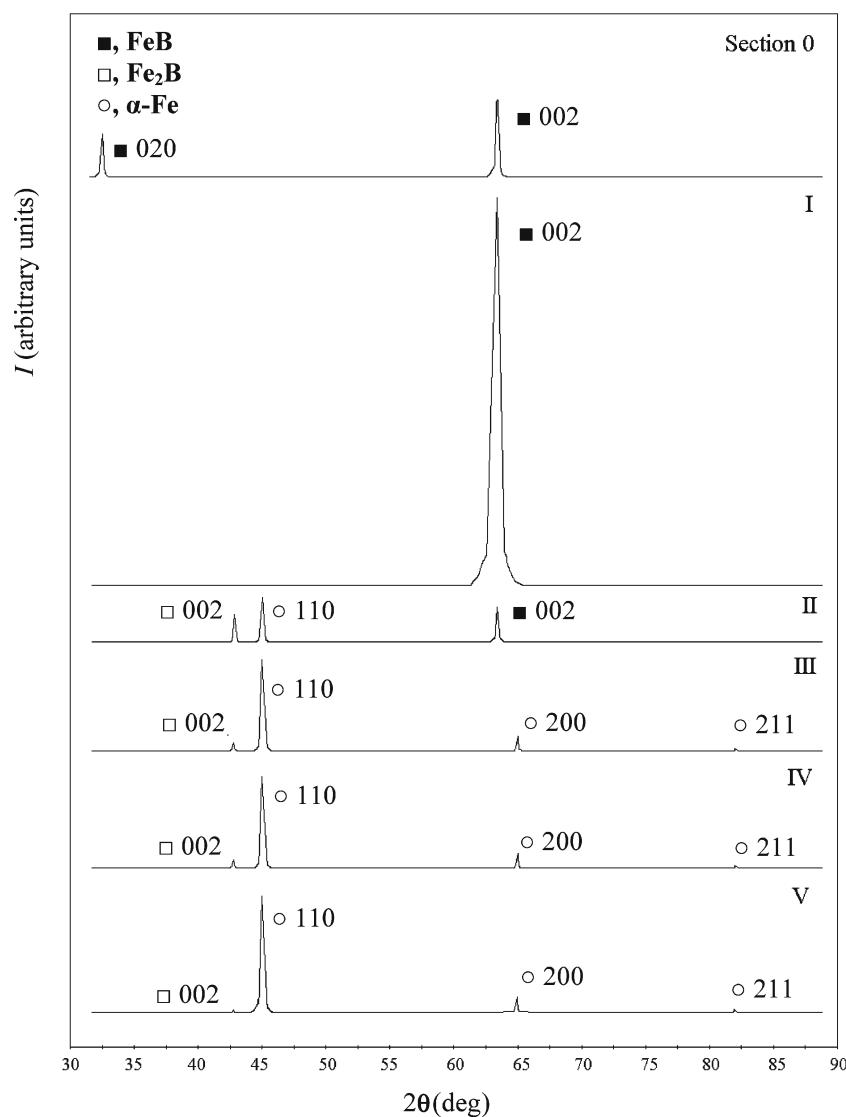


Table 3 X-ray diffraction data showing preferential directions of growth for the FeB and Fe₂B phases formed at the interface between an Fe–25% Cr alloy and boron at 950 °C and a reaction time of 21600 s (6 h) (see also Figs. 1, 2)

Phase	<i>HKL</i>	<i>d</i> (nm)	Peak intensity (arbitrary units)					
			0 ^a	I	II	III	IV	V
FeB	020	0.275	90					
	002	0.148	161	650	77			
Fe ₂ B	002	0.212			65	33	28	10
α -Fe	110	0.201			92	168	185	195
	200	0.143				43	95	97
	211	0.117				24	31	32

^aSerial numbers of appropriate sections of a borided tablet sample by a plane parallel to its flat surface (section 0, I, II and so on, deeper into the sample bulk, see Fig. 2).

252 continuous front thickness was measured, while the separate long crystals of the (Cr,Fe)₂B phase penetrating deep into the alloy base were neglected.

255 It should be noted that, due to a variety of boriding media employed, kinetic data of different authors differ

257 considerably, even for similar alloys or steels. For example, 258 Goeriot et al. [12] reported that a compact boride layer, 259 5 μ m thick, is formed on the surface of a 26% Cr–1% Mn 260 steel sample, borided in activated B₄C powder at 950 °C 261 for 4 h, with separate fine boride needles extending to

Table 4 Fe, Cr and B contents of reacting phases, found by EPMA measurements on X-ray diffraction samples (see also Figs. 2, 3, 5, 6)

Section in Fig. 2	Region	Content (at.%)			Phase
		Fe	Cr	B	
I	Brighter in Fig. 3	25.9	23.9	50.2	(Fe,Cr)B
		29.0	22.9	48.1	
		26.9	21.1	52.0	
		29.2	19.9	50.9	
		33.1	16.2	50.7	
	Darker in Fig. 3	23.7	24.4	51.9	(Cr,Fe)B
		22.0	29.5	48.5	
		17.7	32.2	50.1	
		20.9	29.8	49.2	
		15.0	33.1	51.9	
III	a in Fig. 5	56.6	12.2	31.2	(Fe,Cr) ₂ B
		53.9	11.5	34.6	
		50.0	16.2	33.8	
	b in Fig. 5	18.4	46.8	34.8	(Cr,Fe) ₂ B
		24.2	44.1	31.7	
		19.6	46.8	33.6	
	c in Fig. 5	79.4	20.6	0.0	Fe–Cr
		77.5	22.5	0.0	
		81.9	18.1	0.0	
IV	Brighter in Fig. 6	76.1	23.9	0.0	Fe–Cr
		80.1	19.4	0.5	
		74.2	25.8	0.0	
	Darker in Fig. 6	18.8	49.2	32.1	(Cr,Fe) ₂ B
		19.0	47.0	34.0	
		19.6	50.7	29.7	
V	Brighter in Fig. 6	72.8	27.2	0.0	Fe–Cr
		72.2	27.8	0.0	
		72.5	27.5	0.0	
	Darker in Fig. 6	23.4	43.1	33.5	(Cr,Fe) ₂ B
		18.6	48.7	32.7	
		21.8	45.1	33.1	
VI		73.9	26.1	0.0	Fe–25%Cr
		73.0	27.0	0.0	
		73.7	26.3	0.0	

262 about 50 μm into the steel matrix. In our investigation,
 263 appropriate values for the Fe–25% Cr alloy are 65 μm and
 264 around 120 μm. This great difference appears to arise
 265 mainly from the different potential of boriding agents rather
 266 than from the difference in the chemical composition
 267 of those materials.

268 The growth kinetics of two compound layers are usually
 269 treated using parabolic equations of the type
 270 $x^2 = 2k_1t$, where x is the layer thickness, k_1 is the layer
 271 growth-rate constant and t is time [9, 15, 16]. As seen in
 272 Fig. 9 and Table 5, such equations produce a quite satisfactory
 273 fit to the experimental data obtained. The average values
 274 of layer growth-rate constants are presented in
 275 Table 6.

276 In fact, however, growth kinetics of the FeB and Fe₂B
 277 layers at the diffusional stage of their formation are
 278 somewhat more complicated and may alternatively be
 279 described by a system of two non-linear equations [10, 17]
 280

$$\frac{dx}{dt} = \frac{k_{outer}}{x} - \frac{rg}{p} \frac{k_{inner}}{y} \tag{1a}$$

$$\frac{dy}{dt} = \frac{k_{inner}}{y} - \frac{q}{sg} \frac{k_{outer}}{x} \tag{1b}$$

281 where x is the FeB layer thickness, y is the Fe₂B layer
 282 thickness, k_{outer} is the FeB layer growth-rate constant, k_{inner}
 283 is the Fe₂B layer growth-rate constant, g is the ratio of the
 284 molar volumes of the FeB and Fe₂B compounds,
 285 $p = q = r = 1$ and $s = 2$ (factors from the chemical formulae
 286 of FeB and Fe₂B).

287 An obvious criterion for the applicability of the system
 288 of equations 1 is the constancy of k_{outer} and k_{inner} over a
 289 given range of time, as is the case with both boride layers
 290 (Tables 5 and 6). The value of g necessary for calculation
 291
 292
 293
 294
 295
 296

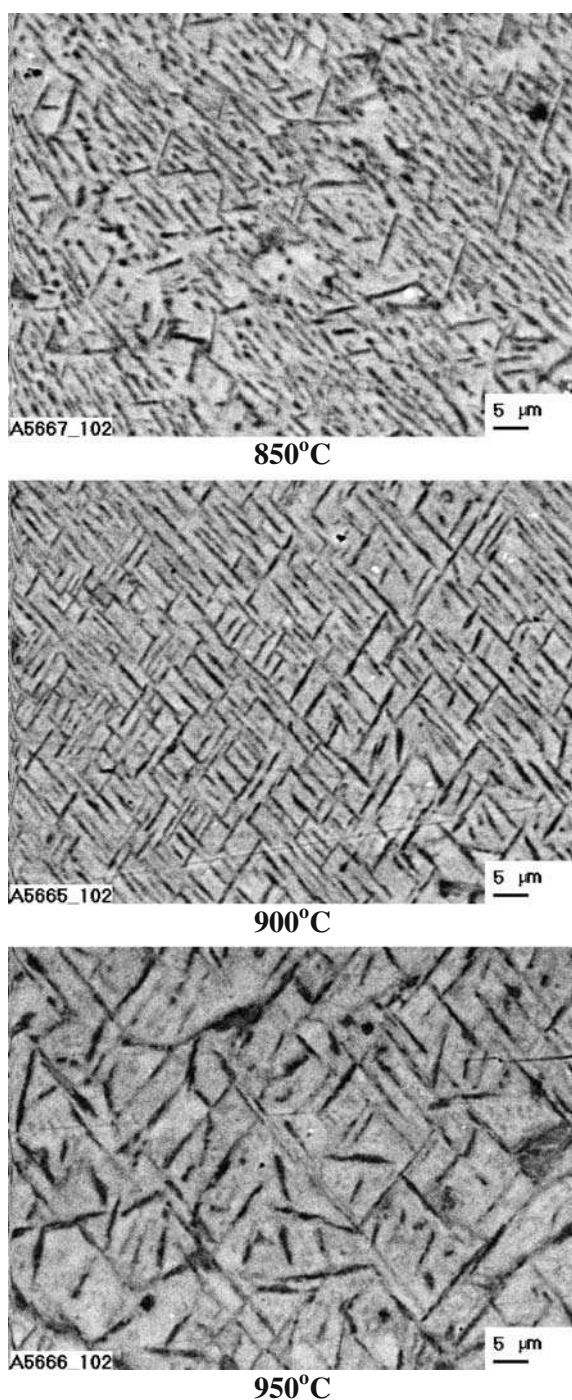


Fig. 5 Plain-view micrographs corresponding to section I in Fig. 2. The brighter regions are the FeB phase enriched in iron, while the darker regions are the FeB phase enriched in chromium

297 tions of k_{outer} and k_{inner} was estimated from the densities
 298 of the FeB and Fe₂B compounds ($6.706 \times 10^3 \text{ kg m}^{-3}$
 299 and $7.336 \times 10^3 \text{ kg m}^{-3}$, respectively [1]) as 0.60. The
 300 derivatives were found from the experimental layer
 301 thickness-time dependences by the numerical three-point
 302 method.

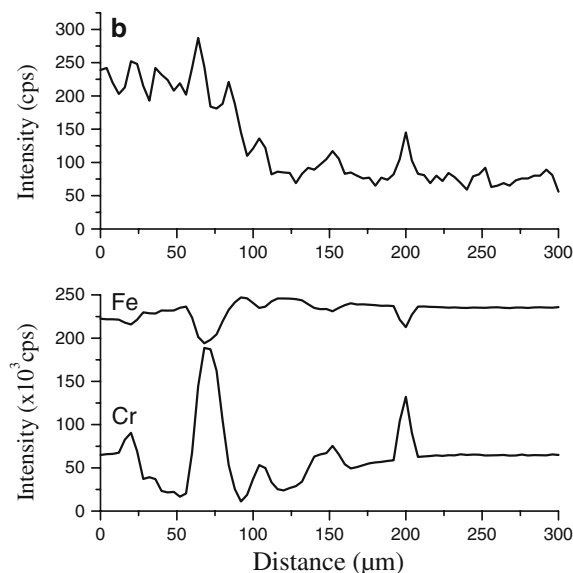
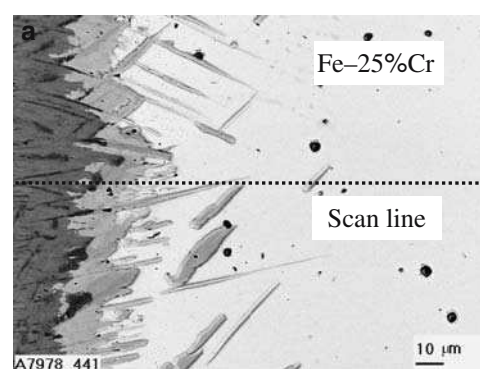


Fig. 6 Microstructure of the transition zone between an Fe–25% Cr alloy and boron and concentration profiles of Fe, Cr and B. Boriding conditions: temperature 950 °C, reaction time 21600 s (6 h)

As seen from Table 5, the results of calculations using
 the system of equations 1 are strongly dependent upon the
 accuracy of measuring layer thicknesses. Approximations
 of experimental data with any suitable analytical functions
 are therefore advisable to obtain more accurate values of
 k_{outer} and k_{inner} . For example, the use of parabolic relations
 to approximate the layer thickness–time dependences and
 then to find the derivatives produces another set of values
 of k_{outer} and k_{inner} (Table 6). Comparing these with the
 average values of k_{outer} and k_{inner} found numerically from
 the experimental points, it may be concluded that both sets
 of the constants agree fairly well, providing evidence for
 the validity of the analytical treatment proposed.

As seen from Fig. 10, the temperature dependence of the
 layer growth-rate constants is described in the 850–950 °C
 range by a relation of the Arrhenius type

$$K = A \exp(-E/RT) \quad (2)$$

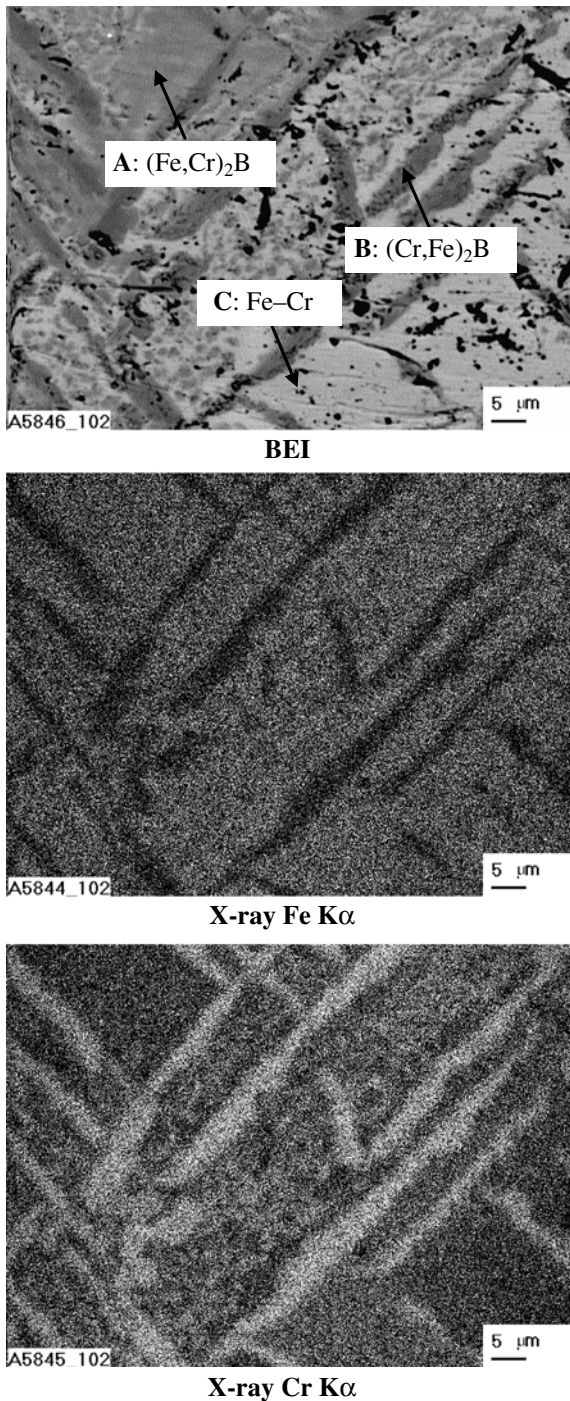


Fig. 7 Plain-view micrograph corresponding to section III in Fig. 2 and X-ray maps for iron and chromium (the brighter the region, the higher is the content of an appropriate element). BEI = backscattered electron image

321 where K stands for any constant, A is the frequency factor,
 322 E is the activation energy, R is the gas constant and T is the
 323 absolute temperature. Application of the least squares fit
 324 method yields the following equations:
 325
 326

$$k_1 = 1.86 \times 10^{-8} \exp(-130.2 \text{ kJ mol}^{-1}/RT) \text{ m}^2 \text{ s}^{-1}$$

for the FeB layer,

$$k_1 = 3.27 \times 10^{-9} \exp(-118.0 \text{ kJ mol}^{-1}/RT) \text{ m}^2 \text{ s}^{-1}$$

for the Fe₂B layer,

$$k_1 = 3.74 \times 10^{-8} \exp(-125.9 \text{ kJ mol}^{-1}/RT) \text{ m}^2 \text{ s}^{-1}$$

for both boride layers,

$$k_{\text{outer}} = 8.07 \times 10^{-8} \exp(-128.3 \text{ kJ mol}^{-1}/RT) \text{ m}^2 \text{ s}^{-1},$$

$$k_{\text{inner}} = 4.32 \times 10^{-8} \exp(-121.7 \text{ kJ mol}^{-1}/RT) \text{ m}^2 \text{ s}^{-1}.$$

Degradation of boride layers during annealing
 in the absence of boriding media

Annealing of a borided Fe–Cr sample (Fig. 11a) in the
 absence of boriding media results in a decrease of the
 thickness of the FeB layer and an appropriate increase of
 the thickness of the Fe₂B layer. As seen in Fig. 11b and c,
 the FeB layer, initially compact and around 40 μm thick,
 disintegrates into separate grains during annealing at
 950 °C and after a 12-h hold disappears almost completely
 as a result of the chemical reaction between iron and FeB
 to form Fe₂B.

This type of consumption is characteristic of non-
 homogeneous layers. Homogeneous layers are usually
 consumed as a whole at their interface with an adjacent
 layer, with their compactness retaining and their thickness
 decreasing. The first phase to disappear is seen in Fig. 11b
 and c to be (Fe,Cr)B because the remaining crystals of the
 outer (Fe,Cr)B–(Cr,Fe)B layer are black. This is confirmed
 by EPMA measurements. The chemical composition of
 black crystals of the outer (Fe,Cr)B–(Cr,Fe)B layer in
 Fig. 11c is 50 ± 2 at.% B, 17 ± 3 at.% Fe and 33 ± 4 at.%
 Cr. Wherever remained between black crystals, the
 (Fe,Cr)B phase has a composition of 50 ± 2 at.% B, 35 ± 3
 at.% Fe and 15 ± 3 at.% Cr. Darker crystals of the outer
 (Fe,Cr)B–(Cr,Fe)B layer have a composition of 33 ± 2
 at.% B, 22 ± 5 at.% Fe and 45 ± 5 at.% Cr. Brighter
 crystals of this layer contain 33 ± 2 at.% B, 25 ± 3 at.% Fe
 and 42 ± 3 at.% Cr.

It should be noted that elongated crystals of the
 (Cr,Fe)₂B phase penetrating deep into the alloy base
 actually do not grow in the absence of boriding media

Fig. 8 Plain-view micrographs corresponding to sections IV and V in Fig. 2. The darker regions are the $(\text{Cr,Fe})_2\text{B}$ phase, while brighter regions are the Fe–Cr alloy base. Black spots are holes and cracks. BEI = backscattered electron image. Magnification: $\times 300$ and $\times 1000$

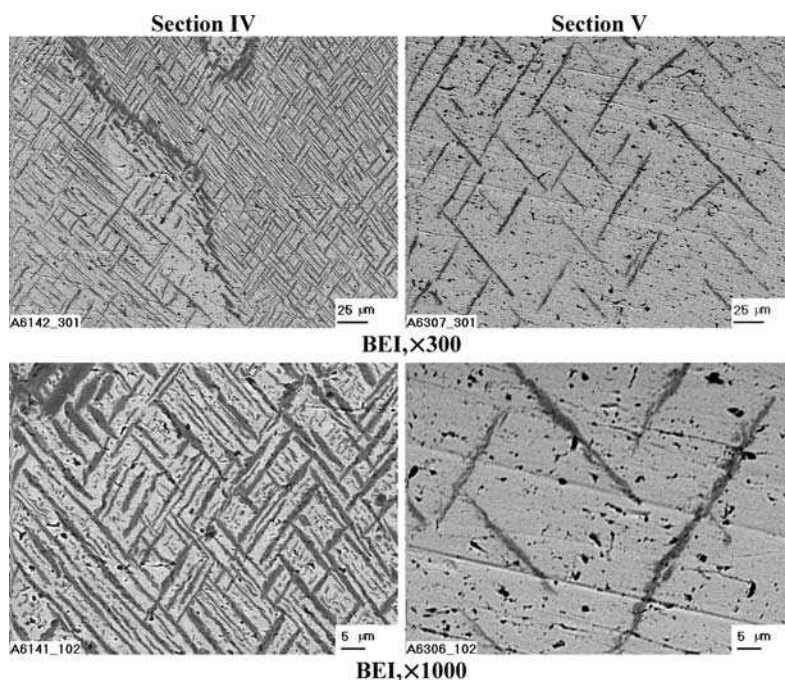


Fig. 9 Plots of layer thickness (left) and squared layer thickness (right) against time for (a) both boride layers, (b) the FeB layer and (c) the Fe_2B layer formed at the Fe–25% Cr alloy–boron interface at a temperature of 850 °C (line 1), 900 °C (line 2) and 950 °C (line 3)

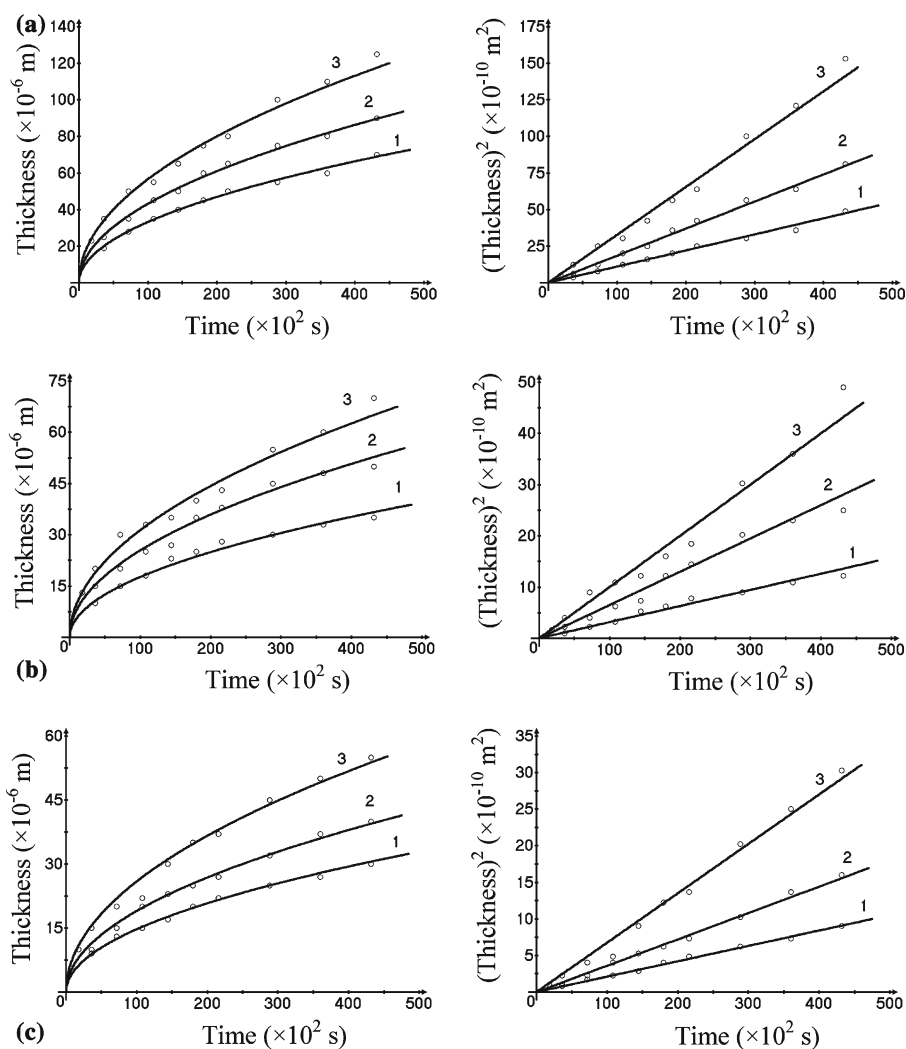


Table 5 Kinetic data for the boride layers formed at the Fe–25% Cr alloy–boron interface

Temperature (°C)	Time ($\times 10^2$ s)	$x(\times 10^{-6}$ m)			$k_1(\times 10^{-14}$ m ² s ⁻¹)			$k(\times 10^{-13}$ m ² s ⁻¹)	
		Total	FeB	Fe ₂ B	Total	FeB	Fe ₂ B	k_{outer}	k_{inner}
850	36	19	10	9	5.0	1.4	1.1		
	72	28	15	13	5.1	1.6	1.2	1.3	1.6
	108	33	18	15	5.0	1.5	1.0	0.93	1.0
	144	40	23	17	5.5	1.8	1.0	1.1	1.1
	180	45	25	20	5.6	1.7	1.1	0.99	1.1
	216	50	28	22	5.7	1.8	1.1	0.85	0.91
	288	55	30	25	5.3	1.6	1.1	0.60	0.68
	360	60	33	27	5.0	1.5	1.0	0.66	0.74
900	36	25	15	10	8.7	3.1	1.4		
	72	35	20	15	8.5	2.8	1.6	1.6	1.6
	108	45	25	20	9.4	2.9	1.9	1.5	1.6
	144	50	27	23	6.9	2.5	1.8	1.7	1.9
	180	60	35	25	8.3	3.4	1.7	2.3	2.1
	216	65	38	27	9.8	3.3	1.7	1.6	1.5
	288	75	45	30	9.8	3.5	1.7	1.8	1.6
	360	80	48	37	8.9	3.2	1.9	1.3	1.5
950	36	35	20	15	17.0	5.6	3.1	3.3	3.3
	72	50	30	20	17.4	6.2	2.8	2.6	2.2
	108	55	33	22	14.0	5.0	2.2	1.8	1.8
	144	65	35	30	14.7	4.3	3.1	2.6	3.2
	180	75	40	35	15.6	4.4	3.4	2.4	2.9
	216	80	43	37	14.8	4.2	3.2	2.7	3.1
	288	100	55	45	17.4	5.3	3.5	3.4	3.7
	360	110	60	50	16.8	5.0	3.5	1.2	1.4
432	125	70	55	18.1	5.7	3.5			

376 (B+KBF₄). The boron atoms released at the interface
 377 between two boride layers, then diffuse across the Fe₂B
 378 layer and react with iron from the alloy base to form more
 379 Fe₂B at the Fe₂B–alloy interface. The thinner the Fe₂B
 380 layer at a certain place, the shorter is the diffusion path and
 381 hence the higher is the supply of diffusing boron atoms to
 382 that place. Therefore, at thinner places the growth rate of
 383 the Fe₂B layer is higher than at thicker ones. As a result,
 384 the Fe₂B–alloy interface flattens with passing time, as
 385 evidenced in Fig. 11b and c.

Table 6 Average values of layer growth-rate constants

Temperature (°C)	$k_1 (\times 10^{-14} \text{ m}^2 \text{ s}^{-1})$			$k (\times 10^{-13} \text{ m}^2 \text{ s}^{-1})$ from experimental points		$k (\times 10^{-13} \text{ m}^2 \text{ s}^{-1})$ from approximated dependences	
	Total	FeB	Fe ₂ B	k_{outer}	k_{inner}	k_{outer}	k_{inner}
850	5.3	1.6	1.1	0.92	1.02	0.86	0.96
900	8.9	3.1	1.7	1.69	1.71	1.60	1.59
950	16.0	5.0	3.1	2.49	2.69	2.63	2.79

386 These experiments clearly show the essential, if not
 387 decisive, role of diffusion of a gaseous boron-containing
 388 phase, probably BF₃ [1, 8, 18], in the course of boriding of
 389 Fe–Cr alloy samples in a mixture of B and KBF₄ under
 390 reduced pressure. Defects of a certain kind and probably
 391 some solid-state transformation in the alloy base, providing

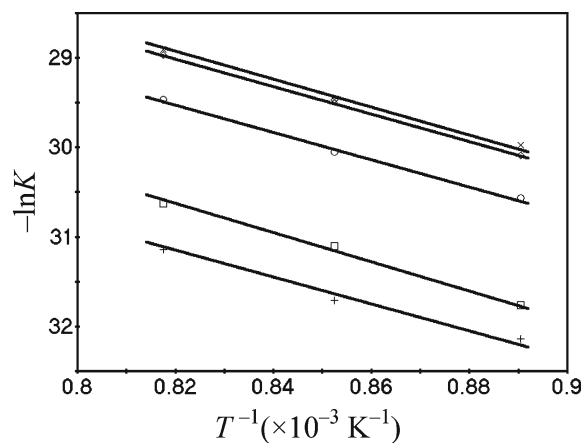


Fig. 10 The temperature dependence of the layer growth-rate constants K : \times , k_{inner} ; \diamond , k_{outer} ; \circ , k_1 for both boride layers; \square , k_1 for FeB; $+$, k_1 for Fe₂B

Fig. 11 Degradation of boride layers during vacuum annealing at a temperature of 950 °C in the absence of boriding media: (a) as-received condition, (b) 6 h annealing and (c) 12 h annealing. BEI = backscattered electron image. Magnification: $\times 300$ and $\times 1000$

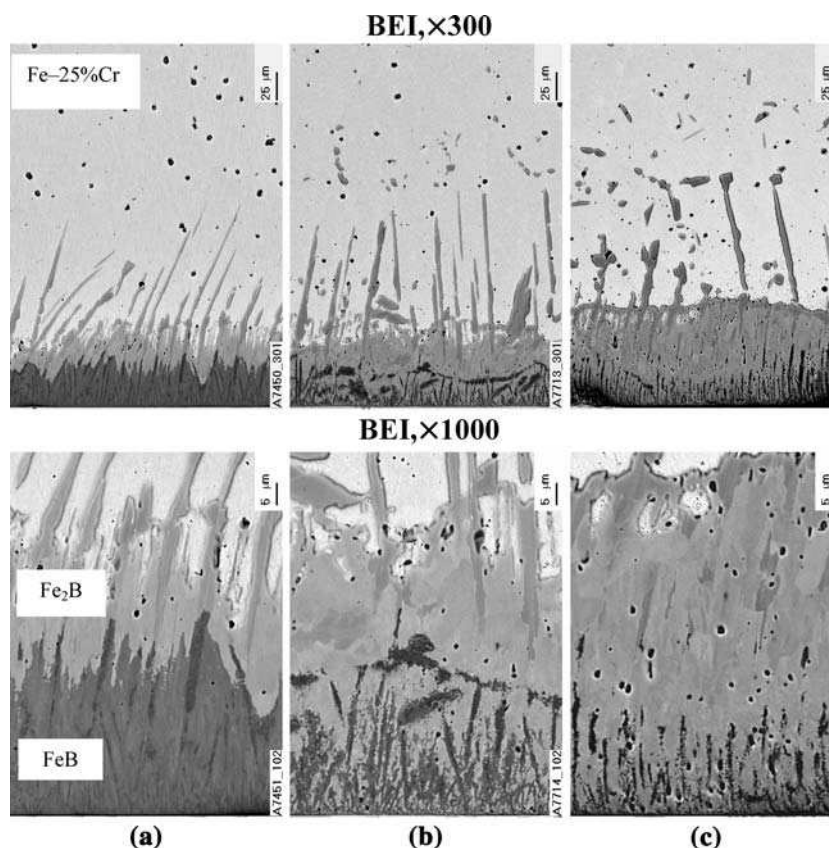


Table 7 Results of abrasive wear resistance tests of borided Fe–Cr alloy samples. Boriding conditions: temperature 950 °C, reaction time 21600 s (6 h)

Borided sample number	Test number	Δm (g) ^a	r^*	Δh (mm)	Phase
111	1	0.00190	154	-0.01	(Fe,Cr)B–(Cr,Fe)B
	2	0.00095	307	<0.01	(Fe,Cr)B–(Cr,Fe)B
112	1	0.00195	150	-0.01	(Fe,Cr)B–(Cr,Fe)B
	2	0.00085	344	<0.01	(Fe,Cr)B–(Cr,Fe)B
113	1	0.00200	146	-0.01	(Fe,Cr)B–(Cr,Fe)B
	2	0.00085	344	<0.01	(Fe,Cr)B–(Cr,Fe)B
		0.29200	1	0.36	Non-borided sample

* r is an increase in wear resistance in comparison with the alloy base

^a Δm and Δh are changes in mass and height, respectively, of tablet samples

392 the paths of rapid diffusion for the gaseous boriding agent,
 393 are responsible for the deep penetration of the (Cr,Fe)₂B
 394 crystals into the sample bulk. It can hardly be solely a
 395 result of the peculiarities of the Fe₂B crystal structure, as is
 396 usually explained [1]. The regular arrangement of the
 397 constituting phases in both boride layers provides evidence
 398 for an additional solid-state transformation. It may either
 399 take place simultaneously with the layer growth or precede
 400 or follow it. This transformation may be closely connected
 401 with the occurrence of hot cracks that boron (>0.007%) is
 402 known to cause in steels at elevated temperatures [19].

Abrasive wear resistance of boride layers

403

Boriding the Fe–Cr alloy tablets for abrasive wear resistance tests was performed at 950 °C for 6 h, producing the (Fe,Cr)B–(Cr,Fe)B and (Fe,Cr)₂B–(Cr,Fe)₂B layers of approximately equal thickness (around 80 μ m in total). Two consecutive tests were carried out on each borided Fe–Cr sample, with each test along a fresh track on emery paper. The results obtained are presented in Table 7, where the data for a non-borided Fe–Cr sample are also given for comparison.

412

413 The wear resistance of the (Fe,Cr)B–(Cr,Fe)B layer,
414 found from mass loss measurements, proved to be 150
415 (outermost portions) to 350 (deeper portions) times greater
416 than that of the alloy base. Somewhat lesser resistance of
417 its outermost portions, compared to deeper ones, is due to
418 both the greater amount of cracks in the near-surface region
419 and a lesser orientation order and hence the compactness of
420 the boride phase.

421 Even though chromium is known to increase the abra-
422 sive wear resistance of steels [1, 18], in the present case the
423 extent of its influence appears to be unexpectedly high.
424 Unlike a Fe–10% Cr alloy, with which three consecutive
425 tests on each sample were sufficient to reach the alloy base
426 [20], it was impossible to do the same with Fe–25% Cr
427 alloy samples, carrying out a reasonable amount of con-
428 secutive tests.

429 Most probably, the great gain in wear resistance of a Fe–
430 25% Cr alloy is due to structural (or morphological) rather
431 than compositional reasons. Further investigations with the
432 use of additional experimental techniques are needed to
433 fully explain this effect.

434 Conclusions

435 Two boride layers based on the FeB and Fe₂B compounds
436 are formed at the interface between a Fe–25% Cr alloy and
437 boron at 850–950 °C and reaction times up to 12 h. The
438 characteristic feature of both layers is a pronounced tex-
439 ture. The strongest reflections are {002} and {020} for the
440 orthorhombic FeB phase and {002} for the tetragonal Fe₂B
441 phase.

442 Each of two boride layers is compositionally two-phase.
443 The outer layer consists of the (Fe,Cr)B and (Cr,Fe)B
444 phases. The inner layer comprises the (Fe,Cr)₂B and
445 (Cr,Fe)₂B phases.

446 Growth kinetics of boride layers is close to parabolic.
447 Alternatively, layer-growth kinetics can be described by a
448 system of non-linear differential equations, also producing
449 a fairly good fit to the experimental data.

450 Annealing of a borided Fe–Cr sample in the absence of
451 boriding media results in the disappearance of the
452 (Fe,Cr)B–(Cr,Fe)B layer, with the (Fe,Cr)B phase disap-
453 pearing first.

454 Microhardness values are 21.0 ± 2.0 GPa for the outer
455 (Fe,Cr)B–(Cr,Fe)B layer, 18.0 ± 1.0 GPa for the inner
456 (Fe,Cr)₂B–(Cr,Fe)₂B layer and 1.35 ± 0.09 GPa for the
457 Fe–25% Cr alloy base.

The abrasive wear resistance of the (Fe,Cr)B–(Cr,Fe)B 458
layer, found from mass loss measurements, is 150 (outer- 459
most portions) to 350 (deeper portions) times greater than 460
that of the alloy base. 461

Acknowledgments This investigation was supported in part by the 462
STCU grant No. 2028. The authors thank V.G. Khoruzha, V.R. Sid- 463
orko, K.A. Meleshevich and A.V. Samelyuk for their help in con- 464
ducting the experiments and carrying out the necessary analyses. 465

References 466

1. Voroshnin LG, Lyakhovich LS (1978) Borirovaniye stali. Met- 467
allurgiya, Moskva (in Russian) 468
2. Kunst H, Schroll H, Luetje R, Wittel K, Lugscheider E, Weber T, 469
Eschnauer HR, Raub C (1991) In: Ullmann's Encyclopedia of 470
Industrial, vol A16. Chemistry Verlag Chemie, Weinheim, p 427 471
3. Sinha AK (1982) In: Sinha AK (ed) Metals handbook, ASM 472
International, Metals Park, OH, p 844 473
4. Hansen M (1958) Constitution of binary alloys, 2nd edn. 474
McGraw-Hill, New-York, p 249 475
5. Vol AE (1962) Stroeniye i svoystva dvoynikh metallicheskih 476
system, vol 1, Fizmatgiz, Moskva, p 679 (in Russian) 477
6. Massalski TB, Murray JL, Bennett LH, Baker H (1986) Binary 478
Alloy Phase Diagrams, vol. 1. American Society of Metals, 479
Metals Park, OH, p 351 480
7. Okamoto H (2004) J Phase Equilibria Diffusion 25:297 481
8. Brandstötter J, Lengauer W (1997) J Alloys Compd 262–263:390 482
9. Gurov KP, Kartashkin BA, Ugaste Yu A (1981) Vzaimnaya 483
diffuziya v mnogofaznikh metallicheskih sistemakh. Nauka, 484
Moskva (in Russian) 485
10. Dybkov I (2002) Reaction diffusion and solid state chemical 486
kinetics (The IPMS Publications, Kyiv) (available for reading at 487
<http://www.i.com.ua/~dybkov/V>) 488
11. Gorelik SS, Rastorguev LN, Skakov Yu A (1970) Rentgenogra- 489
ficheskiy i elektronno-opticheskiy analiz, prilozheniya. Metal- 490
lurgiya, Moskva, p 29 (in Russian) 491
12. Goeuriot P, Fillit R, Thevenot F, Driver JH, Bruyas H (1982) 492
Mater Sci Eng 55:9 493
13. Carbucicchio M, Palombarini G (1987) J Mater Sci Lett 6:1147– 494
1149 495
14. Martini C, Palombarini G, Carbucicchio M (2004) J Mater Sci 496
39:933 497
15. Seith W (1955) Diffusion in metallen. Springer, Berlin 498
16. Hauffe K (1955) Reaktionen in und an festen Stoffen Springer, 499
Berlin 500
17. Dybkov OV, Dybkov VI (2004) J Mater Sci Lett 39:6615–6617 501
18. Voroshnin LG (1981) Borirovaniye promyshlennikh staley i 502
chugunov. Belarus, Minsk (in Russian) 503
19. Motoviln GV, Masino MA, Suvorov OM (1989) Avtomobilnie 504
materialy. Transport, Moskva (in Russian) 505
20. Dybkov VI, Lengauer W, Barmak K (2005) In: Proc 16th Plansee 506
Seminar, Reutte, Austria, May 31–June 4, vol 2, pp 999–1009 507
508